Acta Cryst. (1998). D**54**, 510–521

Structure of a Basic Phospholipase A_2 from *Agkistrodon halys* Pallas at 2.13 Å Resolution

Kehao Zhao,[a] Shiying Song,[a] Zhengjiong Lin[a]* and Yuancong Zhou[b]

[a]*National Laboratory of Biomacromolecules, Institute of Biophysics, Academia Sinica, Beijing 100101, China, and* [b]*Shanghai Institute of Biochemistry, Academia Sinica, Shanghai 200031, China. E-mail: lin@nlblinzj.ibp.ac.cn*

(*Received 10 June 1997; accepted 15 October 1997*)

Abstract

The basic phospholipase A_2 isolated from the venom of *Agkistrodon halys* Pallas (*Agkistrodon blomhoffii* Brevicaudus) is a hemolytic toxin and one of the few PLA_2's capable of hydrolyzing the phospholipids of *E. coli* membranes in the presence of a bactericidal/permeability-increasing protein (BPI) of neutrophils. The crystal structure has been determined and refined at 2.13 Å to a *R* factor of 16.5% ($F > 3\sigma$) with excellent stereochemistry. A superposition of the two molecules in the asymmetric unit gives an r.m.s. deviation of 0.326 Å for all Cα atoms. The refined structure allowed a detailed comparison with other PLA_2 species of known structures. The overall architecture is similar to those of other PLA_2's with a few significant differences. One of which is in the region connecting the N-terminal helix and the Ca^{2+}-binding loop. Unexpectedly, the conformation of the peptide plane Cys29—Gly30 in the Ca^{2+}-binding loop is very different to that of other PLA_2's. The amide NH of Gly30 does not point toward the proposed site for stabilization of the tetrahedral intermediate oxyanion of the substrate analogue. The structure includes four residues which occur less frequently in other PLA_2's. His1, Arg6 and Trp70 located at the interfacial recognition site may play an important role in the interaction with aggregated substrates, while Trp77 contributes to the hydrophobic interactions between the β-wing and the main body of the molecule. This structure analysis reveals that two clusters of basic residues are located at or near the interfacial recognition site, forming an asymmetric positively charge distribution. In contrast to the acidic isoform, the present enzyme is a dimer in the crystalline state. The special phospholipid hydrolysis behaviors are discussed in the light of the structure determined.

1. Abbreviations

PLA_2, phospholipase A_2; *A.h.*, *Agkistrodon halys*; *C. atrox*, *Crotalus atrox*; h.n.p.s., human non-pancreatic secretory; r.m.s., root-mean-square.

2. Introduction

Phospholipase A_2 (E.C. 3.1.1.4) comprises a set of extracellular and intracellular enzymes which specifically catalyze the hydrolysis of the C2 ester bond of 3-*sn*-phosphoglycerides to produce lysophosphatidylcholine and fatty acids in a calcium-dependent reaction. The low-molecular-mass (14 kDa) PLA_2's are mainly classified into two groups, based on sequence and structural homology. Group I PLA_2's includes enzymes from mammalian pancreas and the snake venom of *Elapidae* and *Hydrophidae*. Group II PLA_2's are found in a variety of cell membranes and the snake venom of *Crotalide* and *Viperidoe*. Apart from its primary catalytic function, PLA_2 from snake venom possesses a wide variety of pharmacological activities, such as anticoagulation, hemolysis, platelet-aggregation function, presynaptic neurotoxicity and muscular toxicity. These effects may be independent of catalytic activity (Chewetzoff *et al.*, 1989; Arni & Ward, 1996).

The crystal structures have been determined for various PLA_2's from many species (Dijkstra, Kalk *et al.*, 1981; Keith *et al.*, 1981; White *et al.*, 1990; Holland *et al.*, 1990; Scott *et al.*, 1991; Wery *et al.*, 1991; Fremont *et al.*, 1993; Schevitz *et al.*, 1995). These structures show a high degree of similarity, especially at the enzyme active site, in which a catalytic triad formed by a catalytic water molecule, a histidine, and an aspartate is essentially unchanged. A reasonable catalytic mechanism has been proposed for this enzyme based on the structural knowledge (Scott *et al.*, 1990). A few structures of PLA_2 with presynaptic neurotoxicity, myotoxicity, and platelet function have also been determined (Westerlund *et al.*, 1992; Arni & Ward, 1995; Kwong *et al.*, 1995; Wang *et al.*, 1996).

Three kinds of phospholipase A_2 have been purified from the venom of *Agkistrodon halys* Pallas (*i.e. Agkistrodon blomhoffii* Brevicaudus). They were designated as acidic, neutral and basic PLA_2 according to their isoelectric points (4.5, 6.9 and 9.3, respectively). These isoforms differ significantly in catalytic properties and pharmacological activities. Of the three isoforms, the acidic enzyme shows the highest reactivity toward hydrolysis of monolayers at the air–water interface. The basic enzyme is unique in its behavior toward

ISSN 0907-4449

natural substrates concerning the hydrolysis of *E. coli* membranes in the presence of a bactericidal permeability-increasing (BPI) protein from neutrophil sources (Chen *et al.*, 1987; Forst *et al.*, 1987). The acidic PLA_2 displays the ability to inhibit platelet aggregation (Chen *et al.*, 1987); the neutral PLA_2 designated as agkistrodotoxin, is characterized by potent activity as a presynaptic neurotoxin (Kondo *et al.*, 1989); while the basic PLA_2, in common with some basic PLA_2's from other sources, possesses the ability to hemolyze erythrocytes (Condrea *et al.*, 1981; Shukla & Hanahan, 1981). The basic PLA_2 is highly homologous to the basic PLA_2's from *Agkistrodon halys* Blomhoffii and from *Trimeresurus flavoviridis* (95 and 83% sequence identity, respectively) (Pan *et al.*, 1996; Forst *et al.*, 1986; Kini *et al.*, 1986) which show high anticoagulant activity (Verheij *et al.*, 1980; Kini & Evans, 1987).

A project of crystallographic structure analyses is undertaken, with the hope of understanding the functional differences of these isoforms. The structure of the acidic PLA_2 has been determined by the molecular replacement method and refined at 2.0 Å (Wang *et al.*, 1996). The neutral PLA_2 has been crystallized in several crystal forms (Jin *et al.*, 1990; Li *et al.*, 1995), all of which have multiple copies of molecules in asymmetrical units. The structure has been determined for one of the crystal forms, the $P2_1$ space group, containing eight molecules in an asymmetrical unit (Tang *et al.*, unpublished work). We have previously crystallized the basic PLA_2 in two crystal forms (Meng, Niu *et al.*, 1996; Niu *et al.*, 1995) and made a molecular-replacement study for one of them (Meng, Lin *et al.*, 1996). A new good quality crystal form of the basic PLA_2 was also obtained (Zhao *et al.*, 1997). We report here the structure of this new crystal form of the basic PLA_2 determined by molecular replacement and refined at 2.13 Å to a final R factor of 16.5%. A detailed description of the structure is given with a comparison to related enzymes, especially the acidic PLA_2 from the same venom.

3. Experimental

3.1. *Crystallization and data collection*

The details of isolation and purification of the basic PLA_2 from the venom of *A.h.* Pallas have been published previously (Wu & Chen, 1981). Crystals were grown by the hanging-drop method with 12 mg ml^{-1} of protein, 0.05 *M* CHES buffer (pH 9.5), 0.1 *M* NaCl, 5%(*w*/*v*) PEG 4000 and 10 mg ml^{-1} $CaCl_2$ in 10 µl drops equilibrated against 0.7 ml well solution of 0.05 *M* CHES buffer (pH 9.5), 0.2 *M* NaCl, 10%(*w*/*v*) PEG 4000 and 20 mg ml^{-1} $CaCl_2$. The crystal belongs to the space group $P2_12_12_1$ with unit-cell dimensions a = 97.13, b = 103.69 and c = 23.27 Å with two protein molecules of molecular mass 13 800 Da each in the asymmetric unit, corresponding to a solvent content in the crystal of 42% by volume (Matthews, 1968).

Table 1. *Crystal parameters and diffraction data*

Space group	$P2_12_12_1$
Cell parameters (Å)	a = 97.13, b = 103.69
	c = 23.27
No. of molecule in a.u.	2
No. of observations	29753
No. of unique reflections	12001
Completeness of data (%)	86.2
Resolution (Å)	2.13
R_{merge}† (%)	4.59

† $R_{merge} = \sum |I_i - (I)| / \sum |(I)| \times 100\%$.

Table 2. *Refinement statistics*

R factor (%)†	16.5
R_{free} (%)‡	25.5
Resolution range (Å)	6.0–2.13
Number of reflections ($F > 3\sigma$)	11074
Model	
Number of protein atoms	1916
Number of Ca^{2+} ions	2
Number of water molecules	190
R.m.s. deviations from ideality	
Bond distances (Å)	0.013
Bond angles (°)	2.72
Dihedral angles (°)	23.4
Improper angles (°)	1.29

† $R_{factor} = \sum ||F_o| - |F_c|| / \sum |F_o| \times 100\%$. ‡ 10.45% of the total reflections are used for R_{free} calculation.

A single crystal of the basic PLA_2 with dimensions of 0.3 × 0.6 × 1.2 mm was mounted in a glass capillary. X-ray diffraction measurements were made with a Siemens XRD-100 area detector mounted on a Rigaku RU200 rotating-anode X-ray generator operating at 200 mA and 50 kV (λ = 1.5418 Å). The area detector was placed at 140 mm from the crystal, and the 2θ was set to 20° using $\Delta\varphi = 0.25°$ and an exposure time of 120 s per frame. The data were scaled and merged using the *XENGEN* software (Howard *et al.*, 1987). The overall merged R factor was 4.59% for 29 753 observations of 12 001 reflections. The data set was 86.2% complete to 2.13 Å resolution. The data-collection parameters are summarized in Table 1.

3.2. *Structure solution and refinement*

The orientational and positional parameters of the basic PLA_2 molecules in the unit cell were determined by the molecular-replacement method using the *AMoRe* package (Navaza, 1994). The search model used in the calculation was the R chain of the PLA_2 from the venom of *Crotalus atrox* (1PP2 in the Brookhaven Protein Data Bank; Brunie *et al.*, 1985) with identity of about 57% between the two PLA_2's. The residues that differed

between the two enzymes were initially treated as alanines. The rotation-function search was calculated using the data in the resolution range 10–3 Å with an integration radius of 20 Å. The self-rotation search gave an almost unique solution, which suggested that the two molecules in an asymmetric unit were related by a non-crystallographic twofold axis. The cross-rotation search showed that the top two peaks of the rotation function appeared with correlation values of 18.6 and 16.0 which were significantly higher than the others. One-body and two-body translation functions confirmed that the first two of the rotation search peaks were correct by the signification of the correlation coefficients, and yielded the correct molecular position information. The rigid-body refinement of *AMoRe* resulted in an *R* factor of 42.4% and a correlation value of 55.4%. The initial model, oriented and positioned according to the molecular-replacement solution, was examined on a Silicon Graphics Iris workstation with the program *FRODO/TURBO* (Jones, 1985) and confirmed that the molecular packing in the crystal lattice was reasonable.

The refinement was carried out using the *X-PLOR* program (Brünger, 1992) and without non-crystallographic symmetry restraints. The first step was based on rigid-body least-squares refinement with an initial model consisting of 1622 non-H atoms in 244 residues and using 4809 reflections in the resolution range 8–3 Å ($F > 3\sigma$). The crystallographic *R* value was reduced in 50 successive cycles from 0.42 to 0.39. Refinement of the atomic positions was followed by 100 Powell minimization refinements, resulting in an *R* value of 29.9%. The resolution range was then extended to 2.5 Å (8073 reflections in the resolution range 8–2.5 Å with $F > 3\sigma$). $2F_o - F_c$ and $F_o - F_c$ maps were calculated and examined. The omit maps were used to assist in building the structure. The side chains were adjusted stepwise during the course of the refinement, which gradually reduced the *R* factor. The resolution range was again

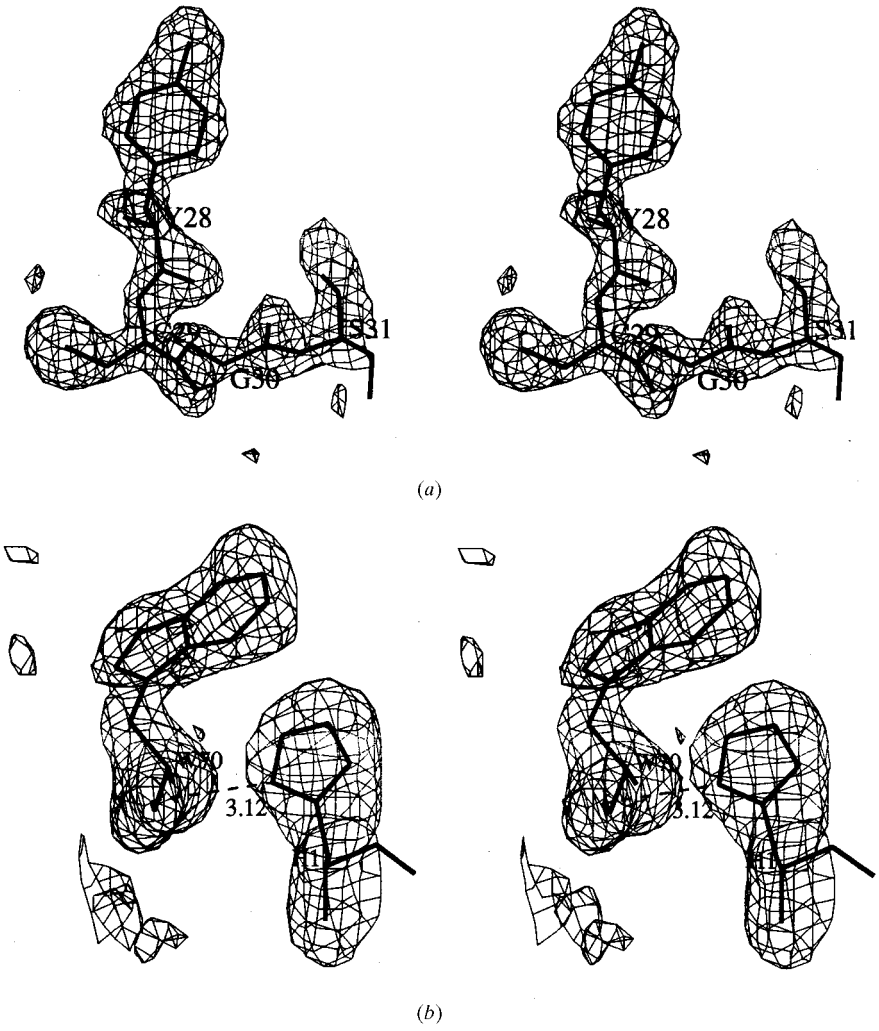

Fig. 1. Quality of electron density at 2.13 Å resolution. The schematic shows the final ($2F_o - F_c$) electron-density map of (*a*) residues 28–31 at the calcium-binding loop, and (*b*) His1 and Trp70. The map is calculated with data 6.0 to 2.13 Å and contoured at the 1.0σ level.

extended to 2.13 Å, and the R factor decreased to 0.23. The model was subjected to simulated-annealing refinement by decreasing the temperature in 25 K steps from an initial value of 3000 to 300 K, with 25 fs of dynamics simulation at each step. Powell minimization, group B-factor refinement, and manipulation of the molecule resulted in a final R value of 0.19. Water molecules were then included in the model if they displayed significant electron density in both $2F_o - F_c$ (contoured at 1.0σ) and $F_o - F_c$ maps (contoured at 3.0σ) and if reasonable hydrogen bonds could be found for the water molecule, and their thermal parameters refined to a value below 70 Å^2. At the end of the refinement, the $F_o - F_c$ map showed no more interpretable features. Table 2 gives the results of the refinement and the quality of the structure.

4. Results

4.1. *Structure quality*

The final model containing 1916 protein non-H atoms, 190 solvent molecules and two calcium ions gives an R factor of 16.5% for reflections in the resolution range of 6.0–2.13 Å and the r.m.s. deviations from ideal stereochemistry of 0.013 Å for bond lengths, 2.72° for bond angles and 23.4° for torsion angles. Based on the Luzzati plot (Luzzati, 1952), the expected coordinate error is found to be approximately 0.25 Å. The electron density corresponding to the polypeptide chain backbones for both molecules in the asymmetric unit are well defined except for residues Ser127 and Ser128 [here we use the nomenclature and numbering scheme of Renetseder *et al.* (1985), see Fig. 6], which are located on the surface of the molecules and have less interactions with the neighboring residues. In addition, the following side chains are partially disordered: Lys11, Lys36, Asp72, Lys129 and Lys132 in molecule A, and Lys11, Glu17, Lys36, Lys78, Lys115, Arg116 and Lys 132 in molecule B. Nevertheless, the structure of these residues and segments could be identified unambiguously (electron-density correlation coefficients of ~0.7), although not as accurately as for the others. An example of fitting between the model and the electron density is presented in Fig. 1. Some differences exist in the sequences of the basic PLA_2 determined by cDNA and chemical methods (Pan *et al.*, 1996). The present structure can resolve the contradictions. For example, X-ray structure indicates a His1 (chemical sequence) rather than a Ser1 (cDNA sequence) on the basis of the appearance of the imidazole ring electron density (Fig. 1*b*), an Ala119 rather than Thr119, and a Leu55 rather than Val55. Furthermore, there is no electron density extending from the Cα atom for residue Arg34 in both molecules (identified by chemical and cDNA), indicating a high degree of disorder for the side chain.

The average temperature factor for all protein atoms is 25.4 Å^2 (23.9 Å^2 for main-chain atoms and 26.9 Å^2 for side-chain atoms). The residues in the active site and the Ca^{2+}-binding site have lower B factors. The B factors for 190 ordered waters range from 8.4 to 66.3 Å^2, with an average of 39.5 Å^2. The average B factors for the main-chain and side-chain atoms of the two molecules in the asymmetric unit are displayed in Fig. 2 as a function of residue number. Regions with B factors exceeding 40 Å^2 include residues 78–80 and 127–129 both in molecule A and molecule B. The electron density for these residues is weak but the tracing of the peptide chain is not ambiguous.

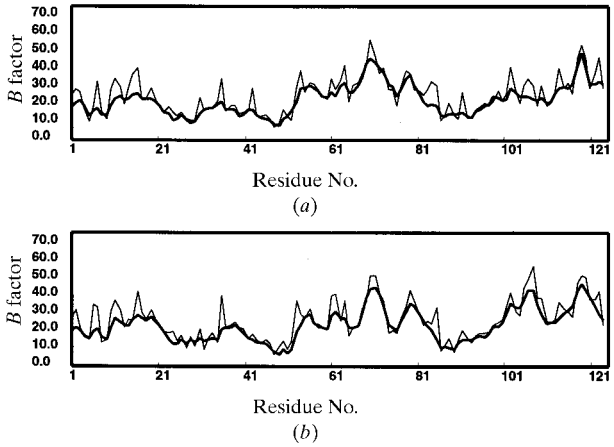

Fig. 2. Plot of the mean temperature factor (Å^2) as function of residue number for all main-chain (thick line) and side-chain (thin line) atoms for (*a*) molecule A and (*b*) molecule B. The molecules are numbered sequentially from 1 to 122.

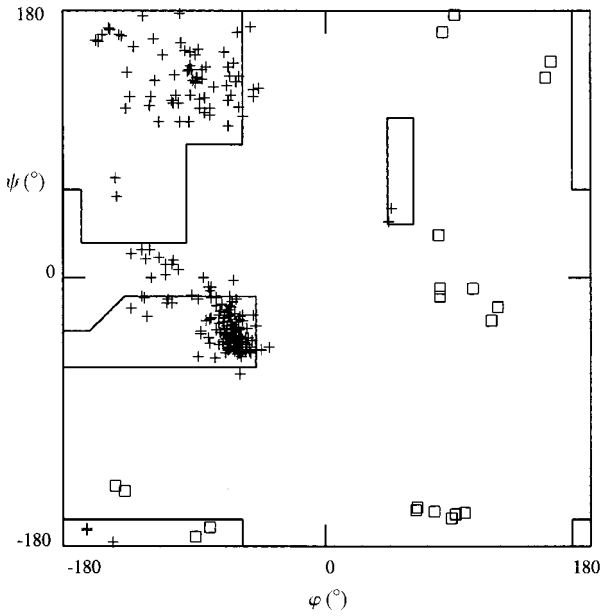

Fig. 3. Ramachandran plot for the basic PLA_2. Glycine and proline residues are denoted by □ and all other residues by +.

A Ramachandran plot (Ramakrishnan & Ramachandran, 1965) as calculated by the program *FRODO/TURBO* is given in Fig. 3. All 210 non-glycine and non-proline residues in the asymmetric unit are located within or very near to the allowed regions.

4.2. *Comparison of the two molecules in the asymmetric unit*

Molecule *B* in the asymmetric unit can be generated from molecule *A* by the following transformation

$$X_1 = 0.10143\text{Xr} - 0.99475\text{Yr} - 0.01393\text{Zr} + 21.71421$$
$$Y_1 = 0.99469\text{Xr} + 0.10165\text{Yr} - 0.01605\text{Zr} - 26.07776$$
$$Z_1 = 0.01739\text{Xr} - 0.01223\text{Yr} + 0.99977\text{Zr} - 5.96772.$$

A superposition of the two molecules in the asymmetric units (Fig. 4) gives r.m.s. deviations of 0.337 Å for all main-chain atoms and 0.326 Å for all Cα atoms. Fig. 5 shows the r.m.s. deviations in positions for all main-chain and side-chain pairs after least-squares superposition of the two molecules. The greatest differences for the main-chain atoms (>1.0 Å) is confined to the fragment consisting of residues 67–71. Since these residues in both molecules have well defined electron densities and main-chain *B* factors of less than 32 Å^2, these large positional differences seem unlikely to be caused by inaccuracy of their coordinates. Closer inspection indicates that this difference may be a consequence of crystallographic environment differences. Fragment 67–71 in molecule *B* has extensive interactions with neighboring molecule *A*, while the corresponding fragment in molecule *A* has much fewer interactions with the neighboring molecule. In addition, residue Ser128 also shows a large deviation (~1.0 Å), which is mostly due to the large coordinate errors since the densities of Ser128 in both molecules are not well defined. If residues Lys69, Trp70 and Ser128 are deleted in the calculation, the r.m.s. deviation drops to 0.266 Å for the 119 Cα atoms, indicating that for most of the chain, the magnitude of the deviation is roughly what is expected from the estimated coordinate errors. Furthermore, the two independent molecules have comparable *B* factors and a similar pattern variation along the chain as shown in Fig. 2, implying excellent correlation to each other. Thus, the structural differences between the two molecules in the asymmetric unit should be disregarded. In the following discussion, only molecule *A* will be analyzed and compared with the PLA_2's unless molecule *B* must be considered.

4.3. *Overall structure*

As expected, the overall structure closely resembles those of other group I/II PLA_2's. The overall fold is characterized by three long α-helices HA (residues 1–14), HC (residues 39–55) and HD (residues 89–109), a short α-helix, HB (residues 17–23), a double-stranded antiparallel β-sheet designated as β-wing (residues 74–85) and a Ca^{2+}-binding loop (residues 25–35). All of these together with the C-terminal ridge are cross-linked by seven disulfide bonds.

The basic PLA_2 molecule containing 122 residues has sequence identity of 63% compared with the acidic PLA_2 from the same venom (group II), 57% compared with *C. atrox* PLA_2 (group II), 52% compared with human non-pancreatic secretory (h.n.p.s.) PLA_2 (group II) and only about 38% when compared with bovine pancreative PLA_2 (group I). Fig. 6 gives the sequence comparison of these enzymes. Disregarding any deletions and insertion in these enzymes, the equivalent set of Cα atoms results in the r.m.s. deviations of 1.06, 1.08, 1.35 and 1.47 Å between the basic PLA_2 and the other four PLA_2's respectively, revealing good correspondence between the structure and sequence identity. The antiparallel long helices *C* and *D* are the structurally most conserved region, as their r.m.s. deviations of corresponding Cα atoms range from only 0.295 to 0.378 Å for this region. Fig. 7 presents the Cα atoms of the present structure superimposed on the acidic PLA_2

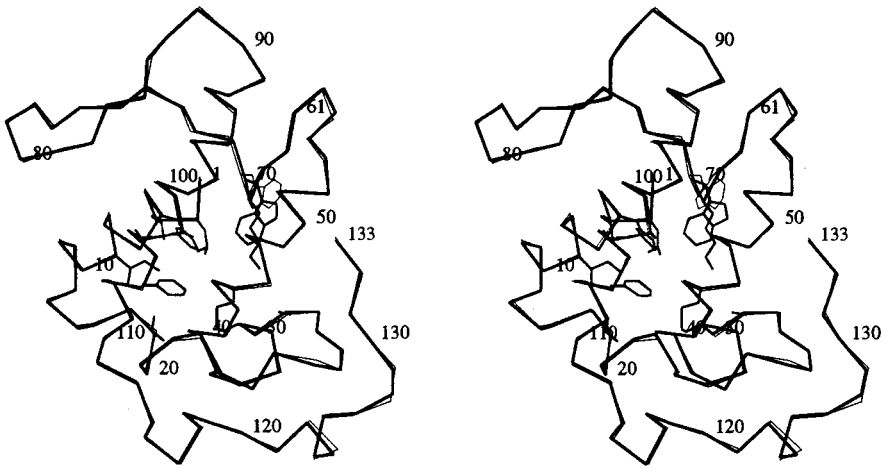

Fig. 4. Stereo diagram showing the superposition of Cα in the two molecules in the asymmetric unit. The thick line represents molecule *A* and the thin line represents molecule *B*. The side chains of the residues around the entrance of the hydrophobic channel are also shown. The side chain of Trp70 is oriented differently in the two molecules. Every tenth residue is labeled.

showing a few regions that have differences. Compared with the acidic PLA_2, the N-terminal helix differs slightly in orientation, the region connecting the N-terminal helix with the Ca^{2+}-binding loop shows significant deviations, the β-wing adopts a slightly closer conformation relative to the main body of the molecule, and the C-terminal ridge from 117 to 133 shows largest positional differences due to the absence of two extra residues.

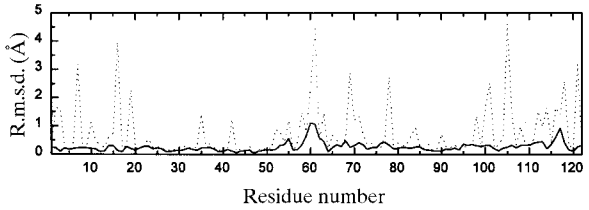

Fig. 5. Differences in main-chain and side-chain position after superimposing molecule *A* and molecule *B*. The r.m.s. differences for the main chain (thick line) and the side chain (dotted line) are shown as a function of residue number.

```
                                1       10        20        30
A.h.pallas  basic               HLLQFRKMIKKMTG-KEPVVSYAFYGCYCG
A.h.blomhoffii  basic           ..............-....I..........
A.h.pallas  acidic              S.I..ETL.M.VAK-.SGMFW.SN......
C. atrox                        S.V..ETL.M.IA.-RSGLLW.SA......
Hnps                            N.VN.HR...LT..-..AAL..G....H..

        40        50        60        70        80        90
SGGRGKPKDATDRCCFVHDCCYEKVT--G-C-----DPKWDDYTYSWKNGTIVCGG-DDP
.........N.....................--.-.-----K.............D.....-...
W..Q.R.Q..............G..--.-.------...M.V.SF.EE..D.....-...
W..H.L.Q..............G.A.--D-.-----N..TVS....EE..E.I...-...
V....S.........VT.....KRLEKR.-.-----GT.FLS.KE.NSGSR.T.AK-Q.S

       100       110       120       130
CKKEVCECDKAAAICFRDNLKTYKK RYMAYPD-ILCS SKSEKC
....I....R.............. .......-.... ......
.........R..........TL.NDKK.W.FGA-KN.PQEE..P.
.GTQI..............IPS.DN K.WLF.P-KD.R EEP.P.
.RSQL........T..AR.KT..N. K.QY.SN-KH.R GSTPR.
```

Fig. 6. The amino-acid sequences of the basic and the acidic PLA_2 from *A.h.* Pallas (Pan *et al.*, 1996; Chen *et al.*, 1987). PLA_2's from *A.h.* Blomhoffii (Forst *et al.*, 1986), *C. atrox* (Renetseder *et al.*, 1985), and human non-pancreatic secretary (Scott *et al.*, 1991) are also shown. The amino-acid residues are numbered essentially according to the common numbering proposed by Renetseder *et al.* (1985). Residues in blank spaces are insertions.

4.4. *Region connecting the N-terminal helix with the Ca^{2+}-binding loop*

Compared with the acidic PLA_2, the short helix HB in this structure extends to include one more residue with the formation of an additional hydrogen bond Val19 O···Ala23 N and an additional water-mediated hydrogen bond Val20 O···Wat···Phe24 N. Immediately following the helix, a type II β-turn between residues 22 and 25 formed with a hydrogen bond Tyr22 O···Tyr25 N. Thus, the peptide segment connecting the N-terminal helix with the Ca^{2+}-binding loop becomes more compact, and the N-terminal helix has a slightly different orientation because of a small swing of its C-terminal end. In the acidic PLA_2, a small piece of three antiparallel β-strands formed around the Ca^{2+}-binding loop and the C-terminal ridge. However, in the basic PLA_2, this conformation is distorted, in which the three peptide groups consisting of residues 24–25, 29–30 and 118–119 are rotated significantly, with the peptide planes approximately perpendicular to the sheet, resulting in the breakdown of the two main-chain hydrogen bonds connecting different strands, *i.e.* Tyr25 N···Cys29 O and Phe24 O···Ala119 N. The conformation in this region in the basic PLA_2 is stabilized by several water-mediated main-chain hydrogen bonds. The peptide group C29—N30 belongs to the Ca^{2+}-binding loop (residues 25–35), which will be described further in next section. Fig. 8 shows the conformational differences of this region compared with the acidic PLA_2.

4.5. *Ca^{2+}-binding site and active site*

In the present structure, the Ca^{2+} ion at the Ca^{2+}-binding site has well defined electron density with a *B* factor of 18.6 $Å^2$. The ion is ligated by the carboxylate O atoms of Asp49 and the carbonyl O atoms of Tyr28, Gly30, Gly32, as well as two water molecules (equatorial and axial water molecules), forming the usual distorted pentagonal bipyramidal structure. The Ca^{2+} ligand distances for the carbonyl O atoms range from 2.33 to 2.36 Å, the distances for the water molecules are 2.39

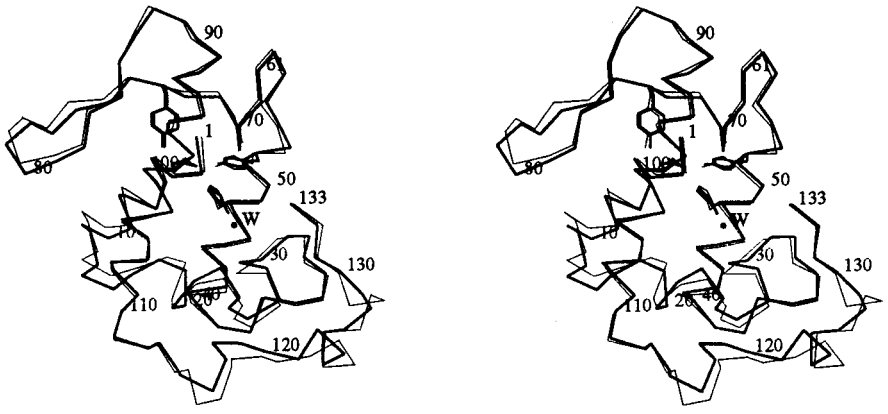

Fig. 7. Comparison of the Cα trace of the basic (thick line) and acidic (thin line) PLA_2. The C-terminal region, the β-wing and the region connecting the N-terminal helix with the Ca^{2+}-binding loop show large deviations. The N-terminal helix is presented in a slightly different orientation (for detail see the text). The active-site residues His48, Asp99, Tyr52, and Tyr73 as well as a catalytic water molecule (•) are structurally conserved and occupy similar positions in both enzymes.

and 2.32 Å, while the distance for both carboxylate O atoms are slightly larger, 2.62 and 2.67 Å.

In the acidic PLA_2 and other Ca^{2+}-binding PLA_2's, the amide NH of Gly30 points toward the Ca^{2+} ion and is stabilized by a hydrogen bond with equatorial water. In the present structure, the flap of the amide group C29—N30 causes the carbonyl O atom of Cys29 to rotate toward the Ca^{2+} ion and hydrogen bonded to the equatorial water. The rotated amide NH of Gly30 in this structure interacts with Tyr25 O and Gly26 O through an intervening water molecule. Fig. 9 shows the structure differences in the Ca^{2+}-binding loop compared with the acidic PLA_2. The flap of the C29—N30 peptide group produced only minor overall conformational changes in the Ca^{2+}-binding loop, as indicated by an r.m.s. deviation of 0.360 Å for the main-chain atoms between the basic PLA_2 and acidic PLA_2. The flap of the peptide group does not result in unreasonable main-chain dihedral angles and variation of the conformation of the disulfide bridge Cys29—Cys45 connecting the Ca^{2+}-binding loop with the helix *C*.

Similar to other PLA_2's, this structure reveals the critical arrangement of the conserved residues His48, Asp99, Tyr73 and Tyr52 and the hydrogen-bonded network formed by their side chains, which are functionally important (Fig. 7). Furthermore, the structure also includes a catalytic triad consisting of Asp99, His48 and a so-called nucleophile attacking water, of which the latter has a well defined corresponding electron density and forms two hydrogen bonds with His48 ND1 and Asp49 OE1 (2.84 and 3.21 Å, respectively). In addition, residues forming the hydrophobic channel for the binding of the phospholipid substrate in PLA_2, *i.e.* Leu2, Leu3, Phe5, Ile9, Val19, Cys29, Ser31, Cys45, Lys69, Ala102, Ala103 and Phe106 are also clearly identified in this structure (Fig. 4). Of these, Leu3, Val19 and Ser31 are different from the corresponding residues Ile3, Met19 and Trp31 in the acidic PLA_2. The side chains of these virtually conserved residues could be superimposable on those of the acidic structure, except for Lys69. The separation between the NZ atoms of Lys69 side chain is about 5 Å, consistent with the suggestion that Lys69 may act as a movable hydrophobic flap and substrate ligand (Scott *et al.*, 1990). All of these indicate that the present structure has the same catalytic mechanism as the acidic and other PLA_2's.

4.6. *Positively charged residues*

The basic PLA_2 is a positively charged molecule with 23 arginines, lysines and histidines and 15 glutamic and aspartic acids. The positively charged residues that could be of importance for phospholipid interactions are unevenly distributed on the surface of the molecule. There are two distinctive basic residue clusters, one at the N-terminal helix which contains five basic residues, and another at a short 3_{10} helix of the C-terminal ridge which contains three consecutive basic residues at positions 114–116.

As shown in Fig. 10, all five basic residues of the N-terminal helix are located on the polar face of the helix and exposed to solvent environment. The concentration of so many basic residues on a face of the N-terminal helix has no effect on the perfect α-helix structure of the functionally important helix as the side chains of these residues adopt different orientations to avoid their charge repellence (the shortest distance between side-chain N atoms of these basic residues is 9.5 Å). In many

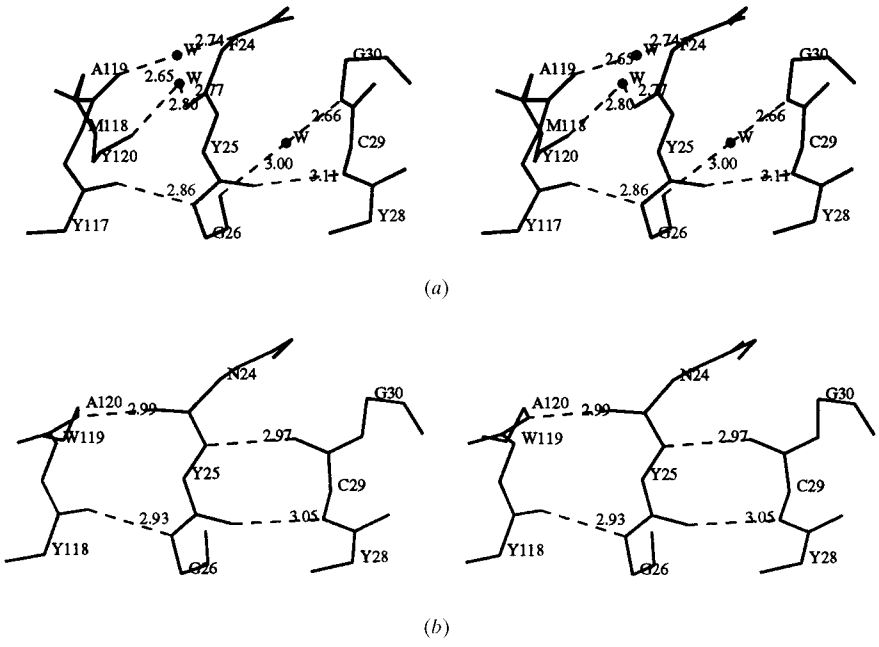

Fig. 8. The region involving three antiparallel β-strands in (*a*) the basic PLA_2, and (*b*) the acidic PLA_2. In the basic PLA_2, a pair of main-chain hydrogen bonds Ala120 O···Asn24 O and Tyr25 N ···Cys29 O were replaced with several water-mediated hydrogen bonds.

other PLA_2 species, the charged residues in the N-terminal helix often form strong polar interactions with the short helix HB and β-wing residues. However, similar interactions have not been found for the present structure. In the basic PLA_2, the NZ atoms of Lys7 and Lys10 form hydrogen bonds with the carbonyl O atoms of residues 3 and 14 from the N-terminal helix itself, thus increasing the stability of the helix. His1 and Arg6 are unusual in known sequences of PLA_2's. This structure reveals that the side chain of histidine at the N-terminus is located at the front of the proposed interfacial recognition site (IRS) (Dijkstra, Drenth *et al.*, 1981). A hydrogen bond formed between the N atom of its imidazole ring and the carbonyl O atom of Trp70 contributes to interactions between the N-terminal helix and a surface loop 67–72 and stabilizes the conformation of this side chain (Fig. 1*b*). The occurrence of an imidazole ring at the N-terminal does not influence the α-helical conformation of the N-terminal residues and the buried feature of the α-amino group, which was reported to play a critical role in interfacial catalysis. The side chain of Arg6, stabilized by weak hydrogen-bond interactions with water molecules, points toward the entrance to the hydrophobic channel with a position similar to that of His6 in uninhibited h.n.p.s. PLA_2. The side chain of Arg6 can be easily rotated out of the entrance and interact with them when binding to the aggregated substrates (Dijkstra, Kalk *et al.*, 1981; Scott *et al.*, 1991). Three basic residues forming a second cluster are also exposed to the solvent environment. Their positively charged side chains are uncompensated.

The charge distribution of the IRS site of the basic PLA_2 is very different from that in the acidic PLA_2. As shown in Fig. 10, in the basic PLA_2, the site (including its edge) contains the five basic residues at the N-terminal helix, five more basic residues at positions 16, 69, 92, 115 and 116 as well as five acidic residues at positions 17, 67, 71, 72 and 122. Therefore, there are five more basic residues than there are acidic residues, and most of the positive charges are located on the left hand side of the

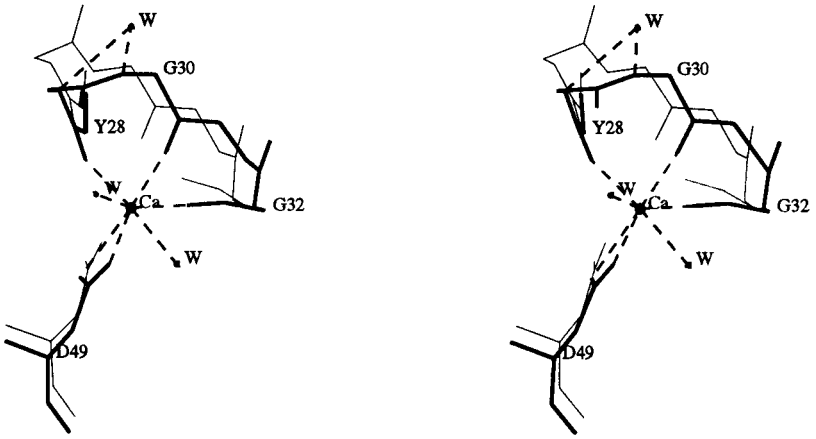

Fig. 9. Stereoscopic comparison of the Ca^{2+}-binding sites of the basic and acidic PLA_2. The difference in the C29—N30 peptide plane orientation is clearly seen.

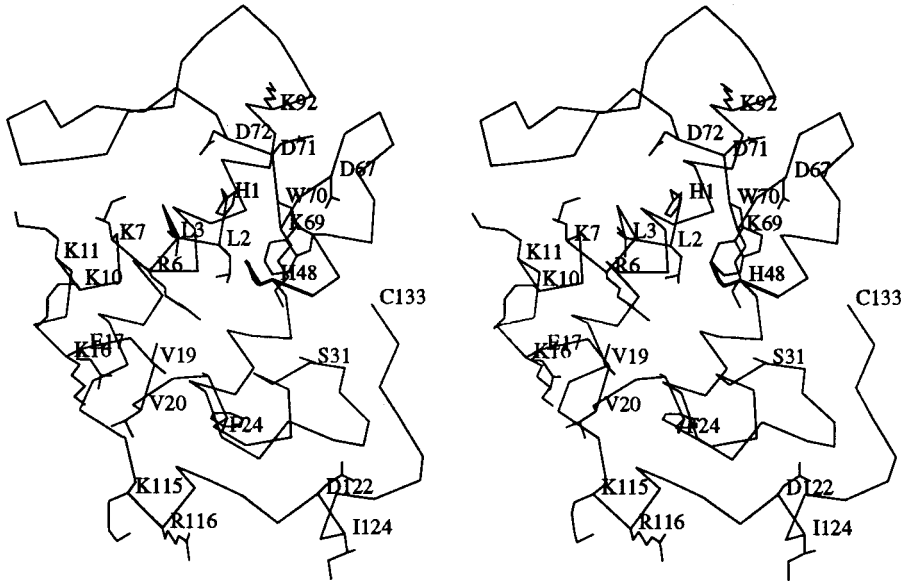

Fig. 10. A stereo diagram showing the residues involved in the putative interfacial binding site for aggregated substrates in the basic PLA_2. The positively charged residues His1, Arg6, Lys7, Lys10 and Lys11 are gathered into a cluster on the polar surface of the N-terminal helix. The side chains of Lys16 and Arg116 may be rotated toward the aggregated substrates when the enzyme binds to them.

channel. The corresponding site of the acidic PLA_2 contains only seven charged residues with only one more basic residue than there are acidic residues. This may account for the differences in phospholipid hydrolysis of the two enzymes and preference of the basic PLA_2 for negatively charged substrates.

4.7. *Two tryptophans*

In the present structure, besides His1 and Arg6 mentioned above, two tryptophans, Trp70 and Trp77, are also less invariant among other PLA_2 species. Residues 31 and 70 located around the entrance to the hydrophobic channel have been suggested to be involved in the interfacial binding site. The acidic PLA_2 has a tryptophan at position 31. In the basic PLA_2, Trp31 is replaced by Ser, but then a tryptophan is present at position 70. This structural analysis indicates that the side chain of Trp70 is present in two conformations with a difference by an approximately 109° rotation about the bond $C^{\beta}-C^{\gamma}$ (Fig. 4), depending on is environment. It could swing outward, making aromatic interaction with tyrosines from neighboring molecule; or may swing inward, toward the entrance to the hydrophobic channel, forming intramolecular interactions. This implies that Trp70 could easily bind to aggregated substrates with its large indole ring increasing the binding ability through enhanced hydrophobic interaction. This observation is consistent with the experimental investigation of the basic PLA_2 by Zheng *et al.* (1996), in which the substrate lecithin caused an obvious change in the tryptophane environment in the presence of Ca^{2+}. Trp77 is inserted between the β-wing and the main body of the molecule, and its indole ring forms hydrophobic interactions with the residues Met12, Ile104, Ile82 and Tyr75 as well as the methylene units of Lys11, where hydrogen-bonding interactions occur in the acidic and other group II PLA_2's (Brunie *et al.*, 1985; Wang *et al.*, 1996). Therefore, Trp77 is involved in the stabilization of this region. Both tryptophans in the present structure play important roles in crystal packing (see next section).

4.8. *Dimer-like structure and crystal packing*

Fig. 11 shows the packing of the basic PLA_2 molecules in the crystal as viewed down along the short *c* axis. There are six contact regions in total. Extensive interactions occur between molecule A' and molecule *B*, which are related by a perfect non-crystallographic twofold axis ($\kappa = 179.9°$). Fig. 12 shows the Cα backbone of this dimer-like structure with residues at the interface. The interactions at the interface involve equivalent residues located in the β-wing, the C-terminal section of the first helix, and the C-terminal ridge. In particular, the side chains of Trp77 in A' interact with the main chains of Asn79 to Gly80 in *B*, and the side chains of Arg107 in A' with the main chains of Met12 to Gly14 in *B*, and *vice versa*, while Leu110–Lys111 interact with their symmetry-related versions. The interactions are mainly hydrophobic in character. The formation of the interface results in the solvent-accessible area buried in the intermolecular interface amounting to 20% (1388 $\AA^2$) of the total area of 7000 $\AA^2$ calculated for an isolated molecule. The interactions also include a few direct hydrogen bonds. The contact region contains a hydrophilic hole, filled with several water molecules, some of which are involved in water-mediated intermolecular interactions. Another important contact region was observed between molecule *A* and molecule *B*. In this region, the side chain of Trp70 from *B* was deeply inserted into the hydrophobic pocket made by residues Tyr120, Tyr117, Arg116 and Leu125 from *A*, while the side chains of Glu53 and Asp71 in *B* formed two salt bridges with the side chains of Lys129 and Arg116 in *A*. In addition, there are two more direct hydrogen bonds and four water-mediated hydrogen bonds. The interactions in the region between A' and B' is similar to that

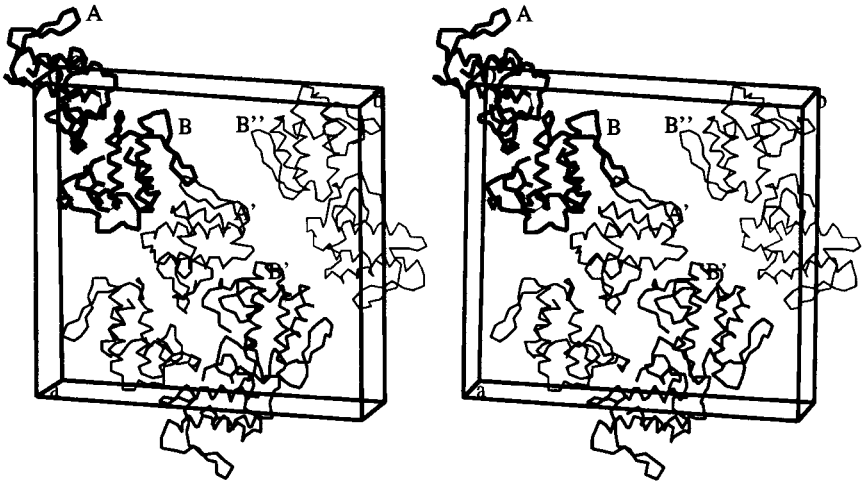

Fig. 11. Stereo diagram illustrating the packing of the basic PLA_2 molecule in orthorhombic crystal. *A* and *B* represent the two molecules in the asymmetric unit; A', B', B'', *etc.*, are the symmetry-related molecules. Crystallographic axes, *a* and *b*, are horizontal and vertical, respectively.

Table 3. *Intermolecular polar interactions*

# Indicates the molecules translated along *c* axis. *A′* and *B′* represent the molecules indicated in Fig. 11.

		Distance (Å)
Molecule *B*	Molecule *A*	
Glu53 OE1	Lys129 NZ	3.12
Glu53 OE2	Lys129 NZ	3.16
Glu53 O	Lys36 NZ	2.86
Asp67 OD2	Tyr117 OH	2.70
Asp71 OD1	Arg116 NH1	3.04
Asp71 OD1	Arg116 NH2	2.91
Molecule *B′*	Molecule *A′*	
Arg116 NH2	Asp71 OD1	3.46
Lys38 NZ	Asp67 OD1	3.05
Molecule *A′*	Molecule *B*	
Asn79 O	Lys11 NZ	2.64
Thr81 OG1	Lys11 NZ	3.37
Arg107 NH1	Lys11 O	3.31
Lys11 NZ	Asn79 O	2.74
Lys11 NZ	Thr81 OG1	3.47
Tyr113 O	Lys111 NZ	3.22
Molecule *A*	Molecule *A*#	
Ser31 OG	Cys133 O	3.44
Ser31 OG	Cys133 OXT	3.00
Molecule *B*	Molecule *B*#	
Ser31 OG	Cys133 O	3.26
Ser31 OG	Cys133 OXT	3.20

between *B* and *A*, but most of them are through water-mediated hydrogen bonds. All the interactions in the contact region between *A′* and *B″* are through water molecules. Ser31 of both *A* and *B* have direct intermolecular interactions with Cys133 of its symmetry-related molecule translated along the *c* axis, which may increase the stability of the Ca^{2+}-binding loop and the C-terminus. The details of the intermolecular direct polar interactions are listed in Table 3.

5. Discussion

Compared with the acidic PLA_2 isoform, the present structure shows the significant conformational differences in the region connecting the N-terminal helix and the Ca^{2+}-binding site. Interestingly, the conformation in this region is more like that of another basic enzyme, h.n.p.s. PLA_2 (Scott *et al.*, 1991), while the conformation in the corresponding region of the acidic PLA_2 is more like those of acidic PLA_2's from *C. atrox* and bovine pancreas. In the basic PLA_2 the peptide group C29—N30 flaps in compared with other PLA_2's as described above. This conformational change has less effect on the coordination geometry of the Ca^{2+} ion. Actually, the pentagonal bipyramidal structure of the Ca^{2+}-binding site of the basic PLA_2 is more perfectly formed than that of the acidic and other PLA_2's. The results presented here seem to indicate that in spite of its almost absolutely conserved sequence, the Ca^{2+}-binding loop in the case of binding a Ca^{2+} ion may show conformational freedom to a certain degree. This is obviously related to the unique sequence of the loop which contains many glycine residues. Although the critical orientation of the peptide is not necessary for the binding geometry of calcium, it may be required by the lipid hydrolysis. In the proposed catalysis mechanism (Scott *et al.*, 1990), the amide NH of Gly30 was suggested to be involved in the stabilization of the transition state. Thus, for the present enzyme, some conformational adjustment of C29–N30 may be required in order to achieve the optimal model for lipid hydrolysis, *i.e.* to eliminate the steric hindrance of the carbonyl O of Cys29 with the substrate and fulfill the stabilization role of the amide NH for the oxyanion of the transition state. The conformational adjustment may occur during the binding of the substrate to the enzyme. The conformational change of C29—N30 may not be a facet of the crystal grown at a high pH value (9.5), as the basic PLA_2 could retain more than 90% activity under this condition (Wu *et al.*, 1985).

It has been suggested that phospholipase A_2's may occlude the substrate-binding sites in some way as a general mechanism for enhancing mobility (Kwong *et al.*, 1995). The Trp31 in the acidic PLA_2 and Arg6 in the basic PLA_2 may play such role, since their side chains oriented toward the entrance to the hydrophobic channel and can be easily rotated out of the entrance and interact with them when binding to the aggregated substrates.

Phospholipase A_2 displays a much higher activity on an lipid–aqueous interface than in solution (Jain *et al.*,

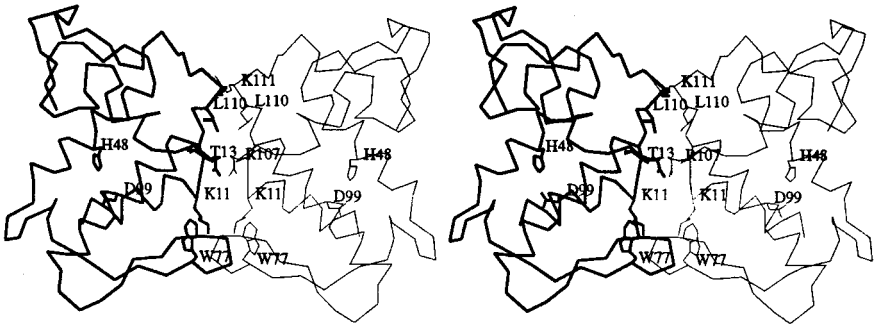

Fig. 12. Stereo drawing of the two independent molecules related by a non-crystallographic twofold axis. Residues involved in the interface are also shown. Molecule *A′* is represented by a thick line, molecule *B* by a thin line.

1993). Dimerization of the enzyme on the membrane surface was supposed to attribute to an increase in catalytic activity (Bell & Biltonen, 1992) and some snake venom PLA_2's exist as dimers in crystal structures (White *et al.*, 1990; Suzuki *et al.*, 1995), and may function as dimers (Brunie *et al.*, 1985; Arni & Ward, 1995). It has been reported that the basic PLA_2 from the venom of *A.h.* Pallas may occur as a dimer in some conditions (Chen *et al.*, 1987). In this crystal structure, two independent molecules are related by a non-crystallographic twofold symmetry (*i.e.* molecule *B* and molecule *A′*, Fig. 12). They look like a dimer structure with a monomer packing different from those of other dimer PLA_2's such as from *C. atrox*, *Trimeresurus flavoviridis* and *Bothrops asper* (Brunie *et al.*, 1985; Suzuki *et al.*, 1995; Arni & Ward, 1995). In the dimer constructions of *C. atrox* and *T. flavoviridis*, the active sites are buried in the interior of the dimer and the substrate has no access to them. Interestingly, in the present structure the two molecules are juxtaposed using the face opposite to that of *C. atrox* and *T. flavoviridis*, thus the active sites are exposed to the exterior. A question arises whether this crystallographic dimer of the basic PLA_2 could exist in physiological conditions as well, and whether the crystallographic dimer reflects different interfacial catalysis behavior from that of the acidic PLA_2, which works as a monomer as evidenced by biological and structural studies (Chen *et al.*, 1987; Wang *et al.*, 1996). Unfortunately, the pH used here for the crystallization is higher than that of physiological conditions. More biochemical and crystallographic work is required to clarify these questions. Determination of the structure of a new crystal form growing under a lower pH conditions is in progress. Nevertheless, the presence of a crystallographic dimer in the basic PLA_2 at least implies a tendency of this enzyme to aggregate.

It was reported that an increase in the net positive charge of the polar face of the N-terminal helix will increase the enzyme activity particularly toward negatively charged substrates in the cases of bovine pancreatic and *C. atrox* PLA_2 (Randolph & Heinrikson, 1982; van Scharrenburg *et al.*, 1982; Forst *et al.*, 1986). The basic PLA_2 from *A.h.* Blomhoffii is highly homologous to the enzyme reported here (only six substitutions, Fig. 6). Compared with most other PLA_2's, these two basic enzymes are unique in their behavior toward natural substrates concerning the hydrolysis of *E. coli* membranes in the presence of BPI protein from neutrophil sources. Based on the finding that four N-terminal lysines, *i.e.* Lys7, Lys10, Lys11 and Lys16 were the most reactive ones in the molecule for this special hydrolytic activity, and that the N-terminal region is a functionally important helix, it was suggested that the cluster of basic residues in this region may be involved in such activity (Forst *et al.*, 1986). This structure analysis provides accurate and detailed structures of these basic residues. According to the description in the previous section lysines at positions 7, 10 and 11 located on the polar face of the N-terminal helix are exposed to the solvent environment, and do not interact with the other structural elements of the molecule. In addition, Lys16 has an uncompensated side chain exposed to the solvent environment. These side chains scatter in different orientations to form a larger positively charged face near the entrance of the hydrophobic channel, which may permit interactions with the negatively charged phospholipid as well as the activator agent (*e.g.* BPI) that facilitates enzyme action (Shier, 1979; Forst *et al.*, 1986).

PLA_2's from different sources or isoforms display different potencies in hemolytic activity due to their structural differences. Of interest is that the acidic PLA_2 showed highest enzyme activity (toward the substrate lecithin) but without hemolytic activity (toward mixture of lecithin and rat or human erythrocyte), while the basic enzyme showed the lowest enzymatic activity but the strongest hemolytic activity. The hemolysis of *A.h.* Pallas PLA_2's was explained as hydrolysis of the substrate lecithin by the enzyme, leading to the release of lysophospholipid. But the hemolytic behavior of these PLA_2's may also be related with different charge distribution on the molecular surface (Wu *et al.*, 1984). Recently, it was shown that when Lys and Arg modified by cyclohexanedione and maleic anhydride, respectively, the hemolytic activity of the basic PLA_2 would only retain 40%, indicating further that this pharmacological activity may be related with some positively charged residues (Zhou, unpublished results). However, the mechanism for hemolysis is still unclear. This structure analysis reveals that two clusters of basic residues are located at or near the interfacial recognition site, forming an asymmetric positively charge distribution. This structural feature is quite different from that of the acidic isoform. It would be interesting to see whether it is related to the functional difference in binding the negatively charged erythrocyte membrane and the hemolytic activity for the two isoforms. Further understanding of this pharmacological activity of phospholipase A_2 requires more extensive biochemical and physical characterization.

We thank Daresbury Laboratory for providing the *CCP*4 suite including the program *AMoRe*. The project was supported by the Science Foundation of the Chinese Academy of Sciences. The data have been deposited in the Brookhaven Protein Bank.†

† Atomic coordinates and structure factors have been deposited with the Protein Data Bank, Brookhaven National Laboratory (Reference: 1JIA, R1JIASF). Free copies may be obtained through the Managing Editor, International Union of Crystallography, 5 Abbey Square, Chester CH1 2HU, England (Reference: GR0679).

References

Arni, R. K. & Ward, R. J. (1995). *Acta Cryst.* D**51**, 311–317.

Arni, R. K. & Ward, R. J. (1996). *Toxicon*, **34**, 827–841.

Bell, J. D. & Biltonen, R. L. (1992). *J. Biol. Chem.* **267**, 11046–11056.

Brünger, A. T. (1992) *X-PLOR Manual*, Version 3.0, Yale University, New Haven, CT, USA.

Brunie, S., Bolin, J., Gewirth, D. & Sigler, P. B. (1985). *J. Biol. Chem.* **260**, 9742–9745.

Chen, Y., Maraganore, J. M., Reardon, I. & Heinrikson, R. L. (1987). *Toxicon*, **25**, 401–409.

Chewetzoff, S., Tsunasawa, S., Sakiyama, F. & Menez, A. (1989). *J. Biol. Chem.* **264**, 13289–13297.

Condrea, E., Fletcher, J. E., Rapuano, B. E., Yang, C. C. & Rosenberg, P. (1981). *Toxicon*, **19**, 705–720.

Dijkstra, B. W., Drenth, J. & Kalk, K. H. (1981). *Nature (London)*, **289**, 604–606.

Dijkstra, B. W., Kalk, K. H., Hol, W. G. J. & Drenth, J. (1981). *J. Mol. Biol.* **147**, 97–123.

Forst, S., Weiss, J., Blackburn, P., Frangione, B., Goni, F. & Elsbach, P. (1986). *Biochemistry*, **25**, 4309–4134.

Forst, S., Weiss, J., Heinrikson, R. L. & Elsbach, P. (1987). *Biochim. Biophys. Acta*, **920**, 221–225.

Fremont, D. H., Anderson, D. H., Wilson, I. A., Dennis, E. A. & Xuong, N. H. (1993). *Proc. Natl Acad. Sci. USA*, **90**, 342–346.

Holland, D. R., Clancy, L. L., Machmore, S. W., Ryde, T. J., Einspahr, H. M., Finzel, B. C., Heinrikson, R. L. & Watenpaugh, K. D. (1990). *J. Biol. Chem.* **265**, 17649–17656.

Howard, A. J., Nielsen, C. & Xuong, N. H. (1987). *Methods Enzymol.* **114**, 452–472.

Jain, M. K., Yu, B. Z. & Berg, O. G. (1993). *Biochemistry*, **32**, 11319–11329.

Jin, L., Gui, L. L., Bi, R. C., Lin, Z. J. & Chen, Y. C. (1990). *Chin. J. Biochem. Biophys.* **4**, 269–276.

Jones, T. A. (1985). *Methods Enzymol.* **115**, 157–171.

Keith, C., Feldman, D. S., Deganello, S., Glick, J., Ward, K. B., Jones, E. O. & Sigler, P. B. (1981). *J. Biol. Chem.* **256**, 8602–8607.

Kini, R. M. & Evans, H. J. (1987). *J. Biol. Chem.* **262**, 14402–14407.

Kini, R. M., Kawabata, S. I. & Iwanaga, S. (1986). *Toxicon*, **24**, 1117–1129.

Kondo, K., Zhang, J., Xu, K. & Kagamiyama, H. (1989). *J. Biochem.* **105**, 196–203.

Kwong, P. D., Mcdonald, N. Q., Sigler, P. B. & Hendrickson, W. A. (1995). *Structure*, **3**, 1109–1119.

Li, D. N., Gui, L. L., Song, S. Y., Lin, Z. J., Qian, Y. & Zhou, Y. C. (1995). *Chin. Sci. Bull.* **40**, 664–667.

Luzzati, V. (1952). *Acta Cryst.* **5**, 802–810.

Matthews, B. W. (1968). *J. Mol. Biol.* **33**, 491–497.

Meng, W. Y., Lin, Z. J. & Zhou, Y. C. (1996). *Sci. Sin.* **11**, 584–591.

Meng, W. Y., Niu, X. T., Gui, L. L., Lin, Z. J., Zhu, H., Zhou, Y. C. & Li, G. P. (1996). *Acta Physicochim. Sin.* **10**, 946–949.

Navaza, J. (1994). *Acta Cryst.* A**50**, 157–163.

Niu, X. T., Meng, W. Y., Gui, L. L., Wang, X. Q. & Lin, Z. J. (1995). *Acta Biochim. Biophys. Sin.* **28**, 206–209.

Pan, H., Ouyang, L. L., Yang, G. Z., Zhou, Y. C. & Wu, X. F. (1996). *Acta Biochim. Biophys. Sin.* **6**, 579–582.

Ramakrishnan, C. & Ramachandran, G. N. (1965). *Biophys. J.* **5**, 909–933.

Randolph, A. & Heinrikson, R. L. (1982). *J. Biol. Chem.* **257**, 2155–2161.

Renetseder, R., Brunie, S., Dijkstra, B. W., Drenth, J. & Sigler, P. B. (1985). *J. Biol. Chem.* **260**, 11627–11634.

Scott, D. L., White, S. P., Browning, J. L., Rosa, J. J., Gelb, M. H. & Siger, P. B. (1991). *Science*, **254**, 1007–1010.

Scott, D. L., White, S. P., Otwinowski, Z., Yuan, W., Gelb, M. H. & Sigler, P. B. (1990). *Science*, **250**, 1541–1546.

van Scharrenburg, G. H. M., Puijk, W. C. & Pieroni, G. (1982). *Biochemistry*, **21**, 6883–6889.

Schevitz, R. W., Bach, N. J., Calson, D. G., Chirgadze, N. Y., Clawson, D. K., Dillard, R., D., Draheim, S. E., Hartley, L. W., Jones, N. D., Mihelich, E. D., Olkowski, J. L., Snyder, D. W., Sommers, C. & Wery, J.-P. (1995). *Nature Struct. Biol.* **2**, 458–465.

Shier, W. T. (1979). *Proc. Natl Acad. Sci. USA*, **76**, 195–199.

Shukla, S. D. & Hanahan, D. J. (1981). *Arch. Biochem. Biophys*. **209**, 668–676.

Suzuki, A., Masueda, E., Yamane, T., Ashida, T., Kihara, H. & Ohno, M. (1995). *J. Biochem.* **117**, 730–740.

Verheij, H. M., Boffa, M. C., Rothen, C., Bryckaert, M. C., Verger, R. & Dehaas, G. H. (1980). *Eur. J. Biochem.* **112**, 25–32.

Wang, X. Q., Yang, J., Gui, L. L., Lin, Z. J., Chen, Y. C. & Zhou, Y. C. (1996). *J. Mol. Biol.* **255**, 669–676.

Wery, J. P., Schevitz, R. W., Clawson, T., Robbitt, J. L., Dow, E. R., Gamboa, G., Goodsoo, T., Hermann, R. B., Kramer, R. M., Mcclure, D. B., Mihelich, E. D., Putnam, J. E., Sharp, J. D., Stark, D. H., Teater, C., Warrick, M. W. & Jones, N. D. (1991). *Science*, **352**, 79–82.

Westerlund, B., Nordlund, P., Uhlin, U., Eaker, D. & Eklund, H. (1992). *FEBS Lett.* **301**, 159–164.

White, S. P., Scott, D. L., Otwinowski, Z., Gelb, M. H. & Sigler, P. B. (1990). *Science*, **250**, 1560–1563.

Wu, X. F. & Chen, Y. C. (1981). *Zool. Res.* **4**, 13–21.

Wu, X. F., Jiang, Z. P. & Chen, Y. C. (1984). *Acta Biochim. Biophys. Sin.* **16**, 664–671.

Wu, X. F., Shi, Q. L., Chen, Y. C. & Lu, Z. X. (1985). *Acta Biochim. Biophys. Sin.* **17**, 507–513.

Zhao, K. H., Song, S. Y., Lin, Z. J. & Zhou, Y. C. (1997). *Chin. J. Biol. Chem.* **13**, 76–80.

Zheng, L., Feng, B., Zhou, Y. C. & Ruan, K. C. (1996). *J. Nat. Toxins*, **5**, 85–93.